JACS
JOURNAL OF THE AMERICAN CHEMICAL SOCIETY
Article
pubs.acs.org/JACS

Gibbs Energy of Superoxide Dismutase Heterodimerization Accounts for Variable Survival in Amyotrophic Lateral Sclerosis

Yunhua Shi,[†] Mark J. Acerson,[†] Alireza Abdolvahabi, Richard A. Mowery, and Bryan F. Shaw*

Department of Chemistry and Biochemistry, Baylor University, Waco, Texas 76798-7348, United States

Supporting Information

ABSTRACT: The exchange of subunits between homodimeric mutant Cu, Zn superoxide dismutase (SOD1) and wild-type (WT) SOD1 is suspected to be a crucial step in the onset and progression of amyotrophic lateral sclerosis (ALS). The rate, mechanism, and ΔG of heterodimerization (ΔG_{Het}) all remain undetermined, due to analytical challenges in measuring heterodimerization. This study used capillary zone electrophoresis to measure rates of heterodimerization and ΔG_{Het} for seven ALS-variant apo-SOD1 proteins that are clinically diverse, producing mean survival times between 2 and 12 years (postdiagnosis). The ΔG_{Het} of each ALS variant SOD1 correlated with patient survival time after diagnosis (R^2 = 0.98), with more favorable ΔG_{Het} correlating with shorter survival by 4.8 years per kJ. Rates of heterodimerization did not correlate with survival time or age of disease onset. Metalation diminished the rate of subunit exchange by up to ~38-fold but only altered ΔG_{Het} by <1 kJ mol^{-1}. Medicinal targeting of heterodimer thermodynamics represents a plausible strategy for prolonging life in SOD1-linked ALS.

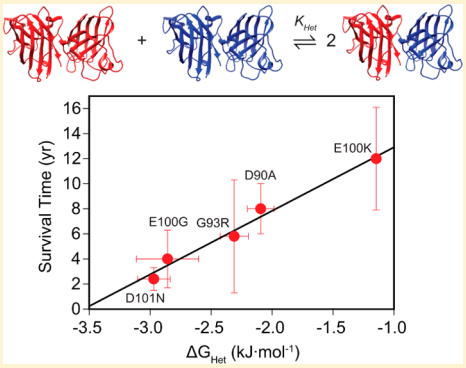

INTRODUCTION

Most of the ~160 mutations in the *SOD1* gene (superoxide dismutase-1) that cause amyotrophic lateral sclerosis (ALS) are autosomal-dominant missense mutations (the D90A mutation is peculiar in that heterozygous D90A mutations cause ALS, except within Scandinavian populations, wherein homozygous D90A mutations cause ALS).[1−3] The wild-type (WT) SOD1 protein, which is isolated from biological systems as a homodimer, is therefore capable of heterodimerization (exchange of subunits) with ALS-variant SOD1 homodimers.[4−6]

Heterodimeric SOD1 has been observed in tissues extracted from ALS patients with heterozygous *SOD1* mutations and in cultured cells that coexpress WT and mutant SOD1.[7−10] The formation of heterodimeric WT mutant SOD1 is hypothesized to account for the puzzling synergy between mutant and WT SOD1 toxicity; that is, expression of WT SOD1 and ALS mutant SOD1 is required for pathogenesis in some ALS mouse models.[10] The rate and free energy of heterodimerization (ΔG_{Het}) have not been determined. Thus, the mechanism of subunit exchange has not been elucidated and categorized as associative, dissociative, or a mixture of two regimes (Figure 1). The absence of the kinetic and thermodynamic values for WT mutant heterodimerization has also prevented researchers from determining whether the kinetics or thermodynamics of heterodimerization correlate with the clinical phenotype associated with each mutation.

Quantifying the rate and free energy of interaction between WT and ALS-variant SOD1 is an important step toward explaining how or why the presence of WT SOD1 can increase the toxicity of ALS-variant SOD1 in vivo.[4,11,12] For example, transgenic mice coexpressing human G93A SOD1 and human WT SOD1 exhibit a more rapid onset and progression of disease as compared to mice expressing only G93A SOD1; similar results are reported for mice coexpressing WT and G85R SOD1.[11,12] Perhaps the strongest indictment of WT SOD1 heterodimerization in familial ALS pathology is the observation that the coexpression of WT SOD1 is requisite for motor neuron disease in the A4V SOD1 transgenic mouse.[13,14] The WT SOD1 protein is, therefore, not likely to represent an innocuous spectator in SOD1-linked familial ALS.[10,15] One way by which WT SOD1 might amplify the toxicity of proteins such as A4V SOD1, an unusually unstable variant that is intrinsically disordered in its disulfide-reduced, metal free state, is that the WT protein might provide a template on which the disordered protein can partially fold or be stabilized.[11,16] The partial folding of an otherwise disordered protein can accelerate certain types of self-assembly.[17,18]

The heterodimerization of ALS-variant and WT SOD1 can occur by three possible mechanisms (Figure 1), none of which are mutually exclusive. In mechanism 1 (the dissociative mechanism), each mutant and WT homodimer must first monomerize, followed by the statistical recombination of homodimers and heterodimers. In mechanism 2 (the associative mechanism), mutant and WT homodimers collide to form an oligomeric intermediate and undergo subunit exchange via molecular reorganization and decay of the

Received: February 16, 2016
Published: April 7, 2016

DOI: 10.1021/jacs.6b01742
J. Am. Chem. Soc. 2016, 138, 5351−5362

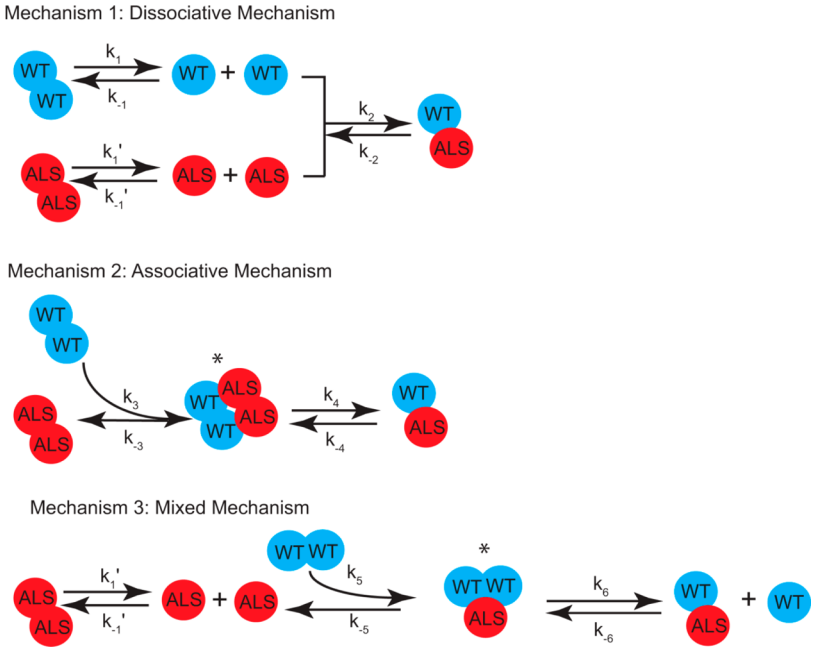

Figure 1. Three possible mechanisms of heterodimer formation from homodimeric wild-type (WT) SOD1 and ALS-variant SOD1 (denoted "ALS"). *The proposed hetero-oligomer stoichiometry shown in mechanisms 2 and 3 was not determined in this study. The smallest possible hetero-oligomer is shown, although higher order oligomers are possible, for example, tetramers of dimers (mechanism 2), or dimers of trimers (mechanism 3).

intermediate (the intermediate is shown as a tetramer in Figure 1, but could be a higher order oligomer such as the octameric "tetramer of dimers" observed by Elam and Hart using X-ray crystallography[19]). In mechanism 3, the "mixed" mechanism, one of the homodimers monomerizes (presumably the dimer that is less stable) and then associates with the opposite homodimer to form a heterotrimeric oligomer (or some other unbalanced oligomer) that decays to a heterodimer. This "mixed" mechanism is especially intriguing because some ALS-variant SOD1 proteins populate monomeric states more so than WT SOD1 (i.e., can exhibit 100-fold greater dimer dissociation kinetics[20,21]), and because trimeric SOD1 has recently been implicated as an especially toxic oligomer.[22]

If subunit exchange occurs under steady-state conditions, which we contend it does under our experimental conditions, then the reaction order will be first order (half order for WT and mutant) regardless of whether mechanism 1 or 2 occurs. If mechanism 3 is predominant (again, assuming steady-state kinetics), then reaction order would be 1.5 (half order for the less stable homodimer and first order for the more stable). Under steady-state conditions, the reaction intermediate (i.e., monomeric or oligomeric SOD1) exists at a low concentration (relative to reactants) and maintains an approximately constant concentration during the reaction. The steady-state approximation is supported by the reportedly low concentration of monomeric SOD1 (or oligomeric SOD1) at ambient conditions (pH 7.4, 22 °C)[23−28] and our inability to detect these intermediates using CE. Thus, mechanism 3 can be implicated or exonerated by simply determining the reaction order; mechanisms 1 and 2 cannot be distinguished by reaction order (see Supporting Information for mathematical proof).

The rate of heterodimerization for WT and ALS-variant SOD1 has not been measured because of the technical difficulties in detecting heterodimers whose subunits differ by only a single amino acid. In this Article, we show that capillary electrophoresis (CE) can be used to measure the rate of heterodimerization between metal-free (apo) WT SOD1 and seven nonisoelectric ALS-variants of apo-SOD1 that span a range of dimer stability (i.e., G93R, D90A, G37R, E100K, E100G, D101N, and N86D SOD1). Capillary electrophoresis is ideal for studying the rate and free energy of SOD1 heterodimerization because it rapidly separates proteins on the basis of their intrinsic net charge and hydrodynamic drag.[29] Heterodimers formed between WT and nonisoelectric mutants, such as E100K, will be readily distinguishable during CE. Unlike gel-based electrophoresis, the measurement of electrophoresis in a bare, fused silica capillary can be performed quickly (<15 min) at high resolution, and the temperature of the capillary can be easily controlled with a liquid-cooled jacket to prevent Joule heating.

In this Article, we are primarily interested in heterodimerization of apo-SOD1 proteins with intact intramolecular disulfide bonds in each subunit (apo-SOD1$^{(S-S)}$) because this state represents the least thermodynamically stable SOD1 dimer[30] and might be the most prone to heterodimerize. Reduction of the disulfide bond in apo-SOD1 results in the least thermostable native state of SOD1, but also leads to monomerization,[24] which by definition disfavors homo- and heterodimerization. Although apo-SOD1 will be largely disulfide reduced in intracellular environments,[31,32] where reduced glutathione varies from ∼0.5 to 10 mM across different organelles,[33] we expect that apo-SOD1 is disulfide-intact after secretion to oxidizing extracellular environments, such as the cerebrospinal fluid (CSF) (where reduced glutathione = 80 nM[34] and where $[SOD1]_{CSF}$ = ∼3 nM[35]). Extracellular environments are venues for the intercellular transmission and propagation of prion-like SOD1.[36−39] The existence of apo-SOD1$^{(S-S)}$ in oxidizing, extracellular environments is almost certain for ALS variants with lowered or abolished metal affinity (e.g., H46R, H48Q, G85R, D125H, D124V, and

DOI: 10.1021/jacs.6b01742
J. Am. Chem. Soc. 2016, 138, 5351−5362

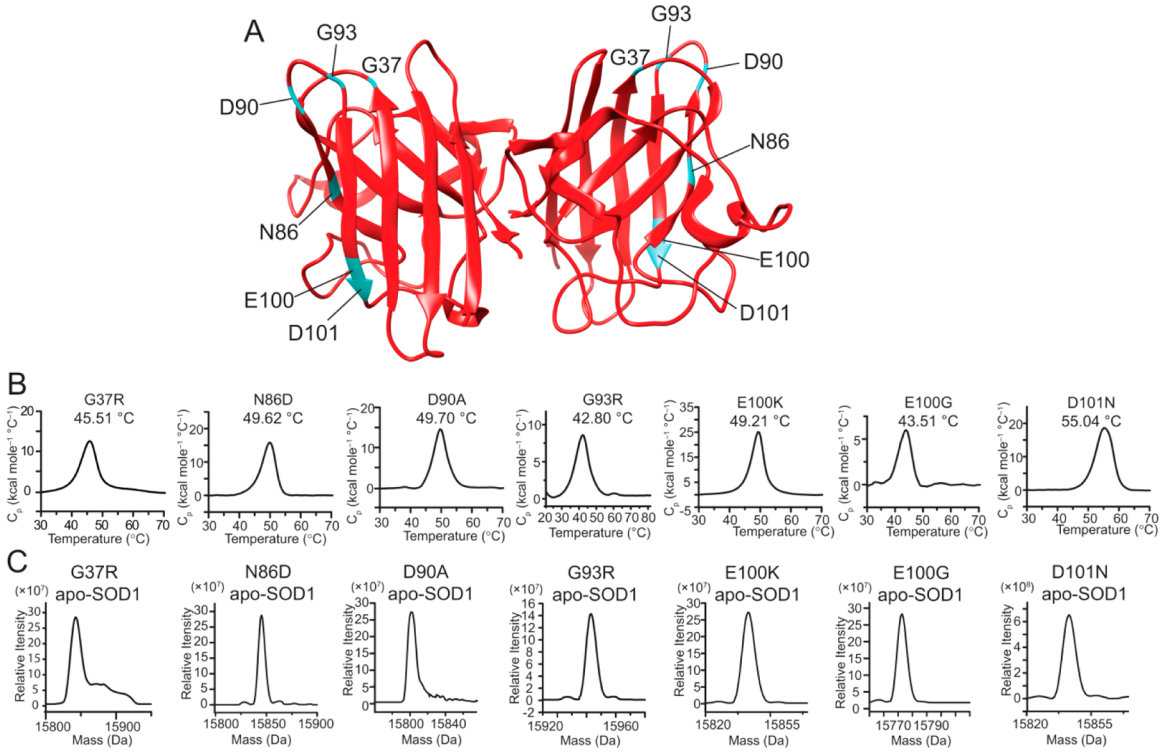

Figure 2. (A) Ribbon structure of Cu, Zn SOD1 (PDB: 2C9V). (B) DSC thermograms and (C) mass spectra for homodimeric ALS-variants of apo-SOD1 analyzed in this study.

S134N SOD1). We are also interested in apo-SOD1$^{(S-S)}$ because apo-SOD1 is a primary constituent of aggregated forms of SOD1 in transgenic ALS mice,[40] and disulfide cross-links are detected in these oligomers[13,41] (which suggests these proteins do not exist in highly reducing environments and/or have buried disulfide linkages).

MATERIALS AND METHODS

Purification, Demetalation, and Remetalation of SOD1. All YEp351-hSOD1 WT and ALS-variant SOD1 plasmids bearing different missense mutations (e.g., D90A, G37R, E100K, E100G, G93R, D101N, and N86D) were transfected into EG118Δsod1 yeast, expressed, and purified using (sequentially) ammonium sulfate precipitation, hydrophobic interaction chromatography, size-exclusion chromatography, and ion-exchange chromatography.[42] All protein concentrations were determined by UV−vis spectrophotometry (λ_{max} = 280 nm and ε = 10 800 cm^{-1} M^{-1}). Proteins were demetalated immediately after purification by sequential dialysis against (i) 0.1 M sodium acetate, 25 mM EDTA, pH 3.8; (ii) 0.1 M sodium acetate, pH 3.8; and (iii) 0.1 M sodium acetate, pH 5.5. The metal content after demetalation was measured with inductively coupled plasma mass spectrometry (ICP-MS), as previously described.[42] Zinc-loaded WT and ALS-variant SOD1 proteins were prepared by gradual addition of a stoichiometric excess (8 equiv per dimer) of zinc sulfate to solutions of apo-SOD1 in sodium acetate buffer, pH 5.5. Solutions were gently stirred at 4 °C. Metalated SOD1 solutions were then transferred into 10 mM potassium phosphate buffer (pH 7.4) via centrifugal filtration. For this buffer transfer, solutions were concentrated 10-fold and diluted 10-fold with 10 mM potassium phosphate, and this cycle was repeated at five iterations. ICP-MS confirmed that all SOD1 proteins were fully metalated (Zn_4-SOD1). No reducing agents were added to apo-SOD1 proteins.

Capillary Electrophoresis of Heterodimeric Apo-SOD1. Capillary electrophoresis was performed within a bare, fused silica capillary using a Beckman P/ACE instrument with a UV detector set at 214 nm. The sample and running buffers were 10 mM potassium phosphate, pH 7.4. The CE analysis of each sample requires <6 min. Heterodimerization was initiated by mixing solutions of homodimeric WT and ALS-variant SOD1 at concentrations ranging from 10−200 μM at 22 °C. Rates and ΔG_{Het} were also measured at 22 °C. Immediately before mixing WT and ALS-variant SOD1, a small amount of DMF (dimethylformamide) was added to each homodimeric solution to function as a neutral marker of electro-osmotic flow ($[DMF]_{final}$ = 1 mM). To measure rates and ΔG_{Het} at 22 °C, ALS-variant and WT SOD1 were analyzed with CE before mixing and after mixing (i.e., 4.5 min after mixing) over the course of 6 h at 22 °C. All homodimeric proteins and CE buffer were warmed to 22 °C before mixing. The protein sample was kept in a storage tray at 22 °C. An autosampler was used to continually inject mixed proteins into the capillary (via pressure injection at 1 psi for 5 s). The temperature of the capillary was maintained at 22 °C by a liquid-cooled jacket surrounding the capillary.

The time point that was recorded for each sample was the time of actual injection of the sample into the capillary (i.e., the beginning of the CE run, as opposed to the end or elution time). This convention was used because heterodimerization between nonisoelectric SOD1 proteins is quenched at the beginning of capillary electrophoresis; that is, although the elution of SOD1 proteins during CE analysis requires ~6 min, WT and ALS-variants SOD1 are immediately separated from one another (at a rate on the order of 8 cm/min) due to their charge differences. Between each measured time point, a series of four additional electrophoresis experiments were performed to wash, recondition, and equilibrate the fused silica capillary for the next measurement. These washing steps were (i) 0.1 M HCl (in Milli-Q water) for 1.5 min (30 psi); (ii) 0.1 M NaOH for 1.5 min (30 psi); (iii) 100 mM potassium phosphate buffer (pH 7.4) for 0.5 min (30 psi); and (iv) 10 mM potassium phosphate buffer (pH 7.4) for 1 min (30 psi).

The electrophoretic mobility (μ) of each species was calculated according to eq 1:

$$\mu = \frac{L_D \cdot L_T}{V}\left(\frac{1}{t_{eof}} - \frac{1}{t}\right) \quad (1)$$

DOI: 10.1021/jacs.6b01742
J. Am. Chem. Soc. 2016, 138, 5351−5362

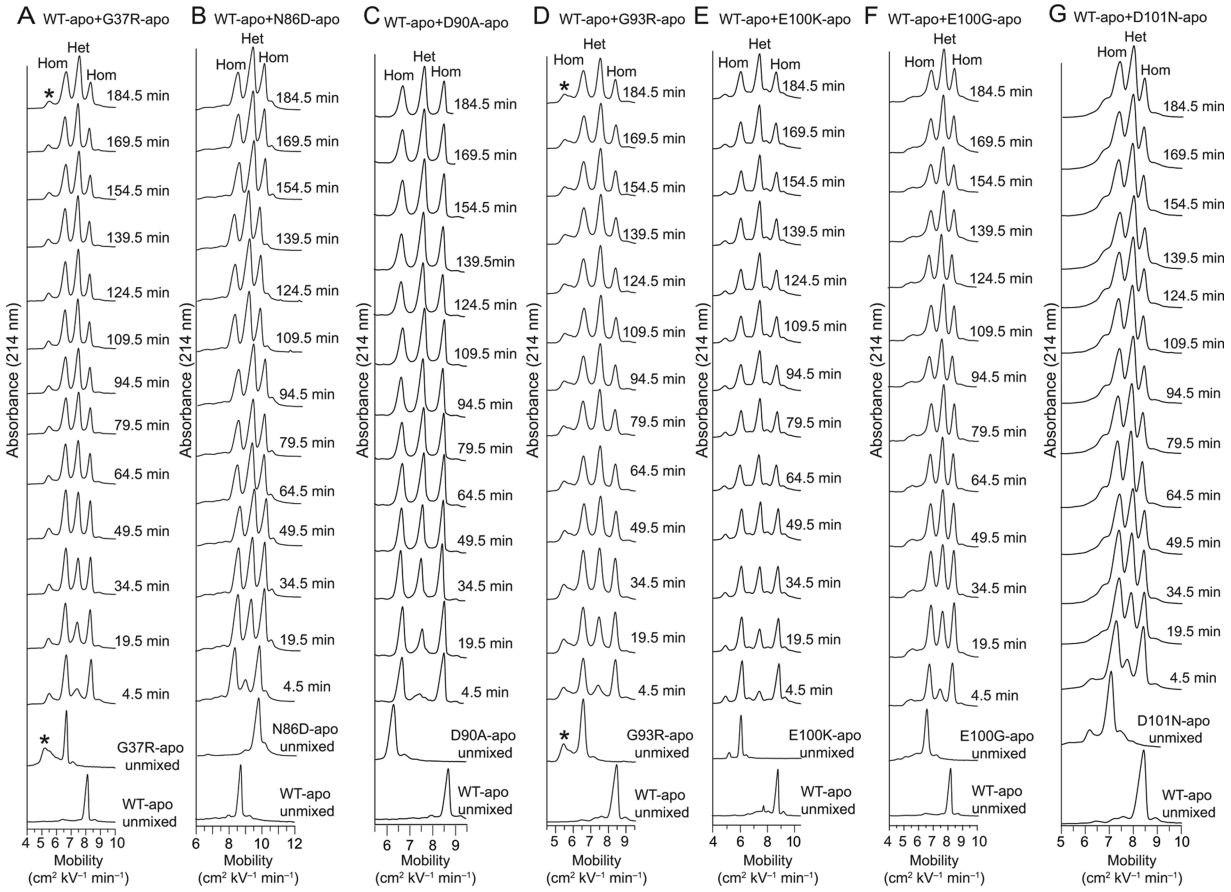

Figure 3. (A–F) Capillary electropherograms of homodimeric WT and ALS-variant apo-SOD1 before and after mixing (heterodimerization); pH 7.4, 22 °C; $[SOD1]_{WT}$ and $[SOD1]_{ALS}$ = 50 μM ($[SOD1]_{Total}$ = 100 μM). Asterisk in electropherograms of G37R (A) and G93R (D) represents unidentified (possibly oligomeric) species.

where L_D is the distance from the inlet to the detector, L_T is the total length of the capillary, V is the applied voltage, t_{eof} is the time required for the neutral marker (DMF) to reach the UV detector, and t is the time required for the protein to reach the UV detector.

Kinetic Analysis of Subunit Exchange. The relative abundance was calculated for WT homodimer, ALS-variant homodimer, and WT/ALS-variant heterodimer using eqs 2, 3, and 4, respectively. The concentration of each protein species was calculated from the area under the curve (AUC) of each peak in the capillary electropherogram. Peak AUCs were determined using a tangent skim with the tangent being defined from approximate local minima to either side of the peak of interest.

$$\%Hom_{WT} = \frac{[Hom]_{WT}}{[Hom]_{WT} + [Hom]_{ALS} + [Het]} \times 100 \quad (2)$$

$$\%Hom_{ALS} = \frac{[Hom]_{ALS}}{[Hom]_{WT} + [Hom]_{ALS} + [Het]} \times 100 \quad (3)$$

$$\%Het = \frac{[Het]}{[Hom]_{WT} + [Hom]_{ALS} + [Het]} \times 100 \quad (4)$$

The relative abundance of WT/ALS-variant apo-SOD1 heterodimer for each reaction was plotted against reaction time and fit to an exponential function to determine reaction order, initial rate, rate constant, and reaction half-life. Moreover, the relative abundance of WT apo-SOD1 homodimer for each reaction was plotted against reaction time and fit to an exponential decay function for a duplicate confirmation of the reaction order.

Differential Scanning Calorimetry. To ensure that apo-SOD1 proteins were properly folded after demetalation, differential scanning calorimetry (DSC) was performed on apo-SOD1 using established protocols.[43] A MicroCal VP-DSC (GE Healthcare) instrument was used, with [SOD1] = 2 mg mL^{-1} (10 mM potassium phosphate buffer, pH 7.4). The scan rate was 1 °C min^{-1} with a scan range of 20–80 °C.

RESULTS AND DISCUSSION

Capillary Electrophoresis of Heterodimeric SOD1. We first examined the purity of homodimeric G93R, D90A, G37R, E100K, E100G, D101N, and N86D apo-SOD1 proteins (Figure 2A). DSC and MS indicated that homodimeric proteins were pure and lacked any post-translational modifications (Figure 2B,C).

All ALS-variant apo-SOD1 proteins exhibited a single predominant peak during electrophoresis that was lower in mobility than the single peak for pure, homodimeric WT apo-SOD1 with the exception of N86D (Figure 3). The lower mobility of these ALS variants of SOD1 is caused by their lower net negative charge, except for N86D, which adds one unit of formal negative charge per subunit and increases mobility. Two SOD1 mutants (G37R and G93R) contained an additional peak in their electropherogram at a lower mobility than their predominant peak (asterisks in Figure 3A,D). These peaks are too abundant to represent metalated SOD1 (ICP-MS analysis showed <0.1 Cu and Zn, per dimeric SOD1) and likely represent oligomeric species. Therefore, to ensure that the concentration of dimeric mutant SOD1 homodimer was identical to that of WT protein, we added a sufficiently high concentration of these mutants to achieve identical integrals of

DOI: 10.1021/jacs.6b01742
J. Am. Chem. Soc. 2016, 138, 5351–5362

WT and mutant homodimers. After mixing ALS-variant and WT apo-SOD1 and immediately repeating CE analysis, a third peak emerged over time with a mobility that was intermediate of each mutant and WT homodimer peak (Figure 3).

We assigned the middle, emergent peak to be the heterodimer of WT and ALS-variant SOD1 (labeled "Het" in Figure 3; homodimers are labeled "Hom"). This peak assignment is justified by the similarity between the measured mobility (μ_{CE}) of each middle peak and the theoretical mobility (μ_{cal}) of each heterodimer as calculated from eq 5 using μ_{CE} and net charge (Z_{CE}) of each homodimer (Table 1). Values of Z_{CE} for G37R and E100G were determined as previously described.[42] Z_{CE} values for homodimers of other mutants and WT SOD1 were determined in previous studies.[42,44]

Table 1. Observed Electrophoretic Mobility for WT and ALS-Variant Apo-SOD1 Homodimers (μ_{CE}), and the Observed and Calculated Mobilities (μ_{cal}) for Each Corresponding Heterodimer

	homodimer	WT/ALS heterodimer	
SOD1 protein	μ_{CE}	μ_{CE}	μ_{cal}
G37R	6.43	8.09	7.41
N86D	9.62	8.98	8.90
D90A	6.39	7.29	7.26
G93R	6.58	7.53	7.51
E100K	5.98	7.41	7.37
E100G	6.69	7.50	7.52
D101N	7.38	7.95	7.90

$$\mu_{Het} = \frac{\mu_{WT}\cdot\mu_{ALS}\cdot(Z_{WT} + Z_{ALS})}{(\mu_{ALS}\cdot Z_{WT}) + (\mu_{WT}\cdot Z_{ALS})} \quad (5)$$

For calculating μ_{Het}, it was assumed that the net charge and hydrodynamic drag of each heterodimer are the sum of the net charge and drag of each subunit. The small differences in the predicted and measured electrophoretic mobility of each heterodimer ($\Delta\mu_{CE\text{-}cal} < 0.68$ cm^2 kV^{-1} min^{-1}) support our assignment of the intermediate peak as the heterodimer of ALS-variant and WT apo-SOD1 (Table 1). For example, the assigned heterodimer peak in electropherograms of WT/N86D had an electrophoretic mobility of $\mu_{CE} = 8.98$ cm^2 kV^{-1} min^{-1}, which differs only by <1% from $\mu_{cal} = 8.90$ cm^2 kV^{-1} min^{-1} (Table 1 and Figure 3).

Mobility values were also calculated for possible short-lived oligomeric species of ALS-variant and WT apo-SOD1 that might form during heterodimerization. Heterotetramer and heterotrimer mobility values ranged from $\mu_{cal} = 6.20$–8.23 cm^2 kV^{-1} min^{-1} and $\mu_{cal} = 6.59$–7.94 cm^2 kV^{-1} min^{-1}, respectively, depending on the ALS-variant involved. Upon examination of the electropherogram, the heterotrimer intermediate did not appear to be present, which suggests that it does not form or

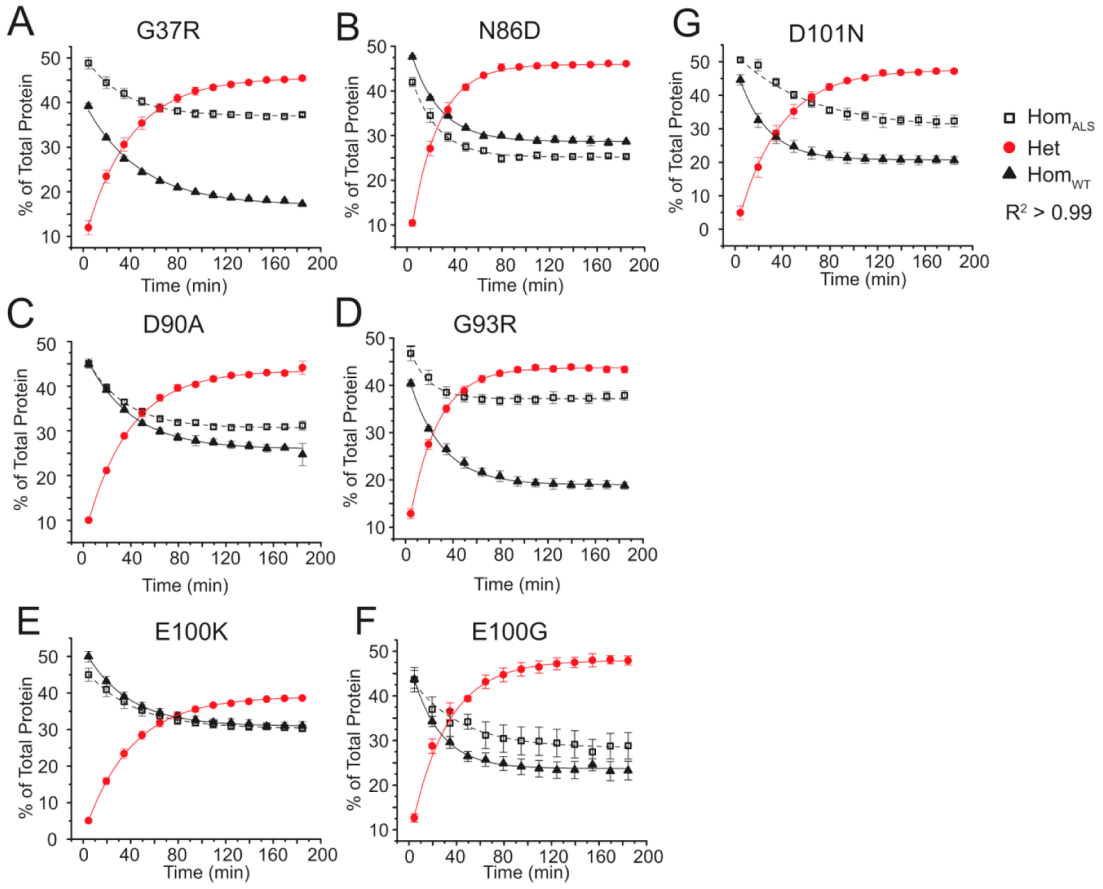

Figure 4. Kinetic plots of heterodimerization for ALS-variant and WT apo-SOD1. The relative abundance of WT and ALS-variant apo-SOD1 homodimers and heterodimer was calculated by integrating the electropherograms in each series from Figure 3. (A–F) Plots of integrated electropherograms of WT and ALS-variants apo-SOD1 homodimers and their respective heterodimers expressed as the % of total protein absorbance at 214 nm. An exponential function (eq 6) was fit to the plot of heterodimer appearance (red ●), and ALS-variant and WT apo-SOD1 homodimer decay (average $R^2 = 0.99$, □ and ▲, respectively).

DOI: 10.1021/jacs.6b01742
J. Am. Chem. Soc. 2016, 138, 5351–5362

that it decays at a rate much faster than the time scale of CE (<7.5 min). The theoretical mobility for each WT/ALS-variant heterotetramer overlaps with the value of its heterodimer, making peak identification for the heterotetramer difficult using CE.

Rate of Subunit Exchange Varies with ALS Mutation. The rate of WT and ALS-variant apo-SOD1 heterodimerization was quantified. Some of these substitutions reduce the conformational stability of the apo-SOD1 dimer (while others do not), in the following order: D101N < D90A ≈ E100K ≈ N86D < G37R < G93R < E100G (Figure 2). We are interested in comparing rates and free energies of heterodimerization as a function of mutant SOD1 thermostability because the thermostability of some ALS mutant SOD1 proteins correlates loosely with clinical phenotypes (i.e., patient survivability).[20] Moreover, several ALS-linked variants with similar thermostabilities have dissimilar phenotypes (e.g., D90A and D101N). We hypothesize that rates or free energies of heterodimerization might explain these discrepancies.

A plot of the diminishing intensity of WT and ALS-variant homodimers and the increasing intensity of WT/ALS-variant heterodimer peak over time is shown in Figure 4A–F. The time points in Figure 4 refer to the time at which samples were injected into the CE instrument after mixing. The rate of heterodimerization for each WT/ALS-variant heterodimer was calculated from the increasing intensity of the heterodimer (Figure 4A–F; red ●). The diminishing intensity of the WT and ALS-variant homodimer peaks (Figure 4A–F; □ and ▲, respectively) offered a parallel means to measure heterodimerization rates. The peak for G37R and G93R homodimers did not diminish as much as peak intensity for homodimers of other mutants, and the WT SOD1 (Figure 4). The most obvious explanation is that the minor peak with low mobility in electropherograms of G37R and G93R (asterisk in Figure 3A,D) is replenishing G37R and G93R via exchanging subunits. This minor satellite peak, which is fascinating in and of itself, and whose low mobility suggests it to be oligomeric, is not present in samples of other mutants, or in WT SOD1.

The exponential function that could be fit to plots of heterodimer or homodimer intensity versus time has the general form of eq 6. Subunit exchange between dimeric WT and ALS-variant apo-SOD1 is, mathematically, a first-order reaction (Figure 4A–F). The rate constant for heterodimerization (k_{Het}, min^{-1}) could be calculated by fitting plots of heterodimer intensity versus time to eq 6. The half-life of the heterodimerization reaction could also be calculated using eq 7. Thus, the formation of heterodimers between ALS-variant and WT SOD1 does not follow the same second-order kinetics commonly observed for dimerization reactions of other biomolecules (e.g., the end-to-end annealing of actin filaments or the annealing of some DNA duplexes), but rather follows first-order kinetics similar to the subunit exchange of higher order multimeric proteins.[45−47] Thus, mechanism 3 is likely not a predominant pathway of heterodimerization.

$$[A] = [A]_0 \cdot e^{-kt} \quad (6)$$

$$t_{1/2} = \frac{\ln(2)}{k} \quad (7)$$

The rate constants and half-lives of heterodimerization for WT and ALS-variant apo-SOD1 are listed in Table 2. These heterodimerization rates were calculated from the appearance of the heterodimer peaks (instead of the disappearance of homodimer peaks) because we know that the initial peak intensity for the heterodimer is zero at $t = 0$. We cannot say, with the same degree of certainty, that each homodimer peak had an intensity of 50% at $t = 0$ relative to one another, and therefore the fitting of any equation to these latter data is less accurate than the former.

Table 2. Kinetic Parameters of Heterodimerization for WT and ALS-Variant Apo-SOD1 at 50 μM Homodimer, pH 7.4, 22 °C[a]

ALS-variant and WT SOD1 mixture[b]	rate constant (k_{Het}; 10^{-2} min^{-1})	half-life ($t_{1/2}$; min)	rate (μM min^{-1}) at $t = 0$ min
G37R + WT	3.74 ± 0.27	18.67 ± 1.43	1.24
N86D + WT	2.37 ± 0.22	29.51 ± 2.60	1.92
D90A + WT	3.63 ± 0.20	19.15 ± 1.07	1.08
G93R + WT	2.36 ± 0.09	29.48 ± 1.19	1.75
E100G + WT	3.04 ± 0.03	22.75 ± 0.28	1.78
E100K + WT	3.89 ± 0.41	18.11 ± 2.07	1.19
D101N + WT	3.66 ± 0.04	19.29 ± 2.39	2.44

[a]Values are shown as mean ± SD ($n = 3$). [b][WT homodimer] = 50 μM; [ALS-variant homodimer] = 50 μM (achieved by adding sufficient protein to produce homodimer peak of area equal to WT homodimer peak).

The rate constant of ALS-variant homodimer did not correlate (linearly or exponentially) with the measured thermostability of each ALS-variant apo-SOD1 homodimer ($R^2_{linear} = 0.25$; $R^2_{exponential} = 0.37$). However, the fastest ALS-variant homodimer decay was observed for E100K SOD1 (a very stable dimer) with $k_{Mu} = 3.89 \pm 0.41$ min^{-1}; the slowest was observed for G93R (a very unstable dimer) with $k_{Mu} = 2.36 \pm 0.09$ min^{-1}. One-way ANOVA analysis was performed for the set of ALS-variant rate constants and yielded $p = 0.0004$, indicating a statistically significant difference between the rate constant of each ALS-variant (Table 2).

The different rates of heterodimer formation for SOD1 mutants ($\Delta[Het]/\Delta t$, μM min^{-1}) were also expressed and illustrated by the difference in the initial reaction rates (extrapolated to $t = 0$ min) for each mutant (Table 2).

To identify the individual order of each reactant (as opposed to the overall order), we measured the rate of heterodimerization for WT and E100K apo-SOD1 as a function of WT and E100K apo-SOD1 concentration (Figure 5). We chose E100K for the concentration-dependent experiment because this variant is the most easily resolved from WT protein during CE (because of its low net charge).

The relevant peaks from electropherograms in Figure 5 were then integrated and fit to eq 6 to calculate rate constants and extrapolate the initial reaction rate (i.e., at $t = 0$ min) for each E100K concentration (Figure 6).

The rate of heterodimer formation is not dependent solely on the concentration of either E100K or WT apo-SOD1 (i.e., eqs 8a and 8b are invalid expressions of SOD1 heterodimerization) as demonstrated by the small increase in reaction rate that accompanied large increases in the concentration of either WT or E100K apo-SOD1 (Figure 7A). Specifically, a 10-fold increase in the concentration of WT or E100K increased the rate of heterodimerization by only ~2-fold. For example, the rate of heterodimerization was 0.27 μM min^{-1} when [E100K] and [WT] were each present at 10 μM. When [E100K] was increased to ~100 μM, the rate only increased to 0.58 μM min^{-1}. Similarly, when [WT] was increased to 100 μM, the measured reaction rate was 0.49 μM min^{-1} (Figure 7A). The

DOI: 10.1021/jacs.6b01742
J. Am. Chem. Soc. 2016, 138, 5351−5362

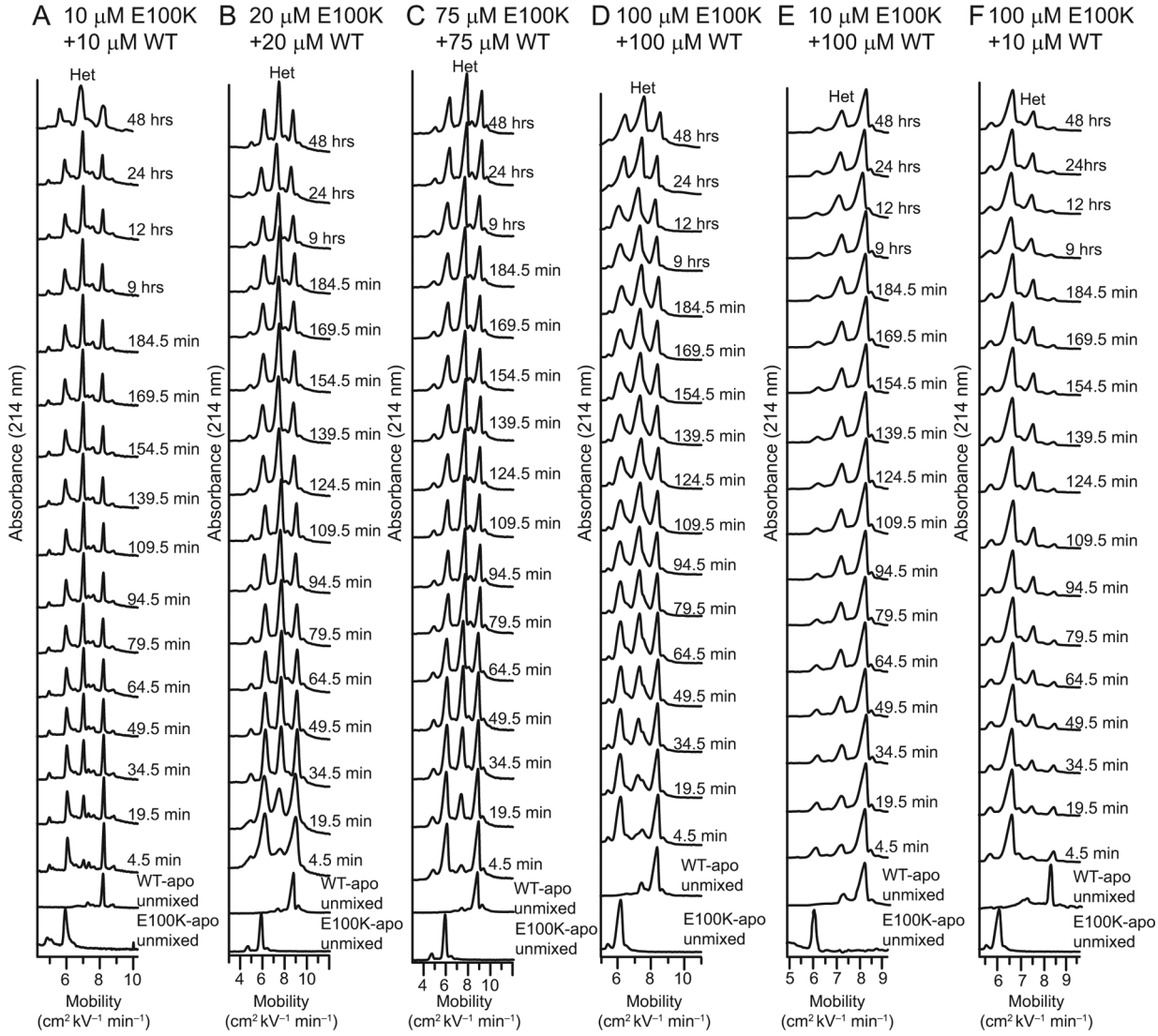

Figure 5. (A–F) Capillary electropherograms of heterodimerization reactions between E100K and WT apo-SOD1 over time at varying concentrations of E100K and WT apo-SOD1 (pH 7.4, 22 °C). In the bottom two electropherograms of each stack (i.e., in electropherograms of homodimers, prior to mixing), the peak intensity of each homodimer was normalized for visual clarity.

observed rate at 110 μM $[SOD1]_{total}$ differs from the predicted rate of 3.60 μM min^{-1} (assuming that the reaction is first order with respect to either of the reactants, according to eqs 8a or 8b). This nonlinear relationship between SOD1 concentration and rate indicates that heterodimerization is not first order with respect to either WT SOD1 or ALS-variant SOD1; that is, this result confirms that the reaction is not second order overall.

$$\frac{\Delta[\mathrm{Het}]}{\Delta t} = k_{\mathrm{Het}}\cdot[\mathrm{E100K}] \tag{8a}$$

$$\frac{\Delta[\mathrm{Het}]}{\Delta t} = k_{\mathrm{Het}}\cdot[\mathrm{WT}] \tag{8b}$$

$$\frac{\Delta[\mathrm{Het}]}{\Delta t} = k_{\mathrm{Het}}\cdot[\mathrm{E100K}]^{1/2}\cdot[\mathrm{WT}]^{1/2} \tag{8c}$$

Assuming instead that the rate is half-order with respect to both reactants, that is, first-order reaction kinetics overall, we plotted the reaction rate ($\Delta[HET]/\Delta t$) against the product of the square root of the concentration of each reactant (Figure 7B). This plot yielded a linear relationship defined by eq 8c. The rate constant of heterodimerization, k_{Het}, is the slope of this plot. The linear fit produced a rate constant $k_{Het} = 3.34 \pm 0.30 \times 10^{-2}$ min^{-1}, with $R^2 = 0.96$ (Figure 7B). This value of k_{Het}, from the plot of $[E100K]^{1/2}\cdot[WT]^{1/2}$ versus $\Delta[HET]/\Delta t$ (Figure 7B), is within the error of average values of k_{Het} calculated from the fit of E100K + WT electropherograms listed in Table 2 ($k_{ave} = (3.89 \pm 0.41) \times 10^{-2}$ min^{-1}).

These similarities further validate our conclusion that heterodimerization of SOD1 follows overall first-order kinetics, with half-order for each WT and ALS-variant protein. These types of nonclassical first-order heterodimerization reactions have been observed for other proteins.[45,46]

The exponential decay function used to fit the kinetic data for each ALS-variant/WT mix was extrapolated to calculate ΔG_{Het}; that is, the plateau of each curve in Figure 4 is proportional to the ΔG_{Het} for that mutant. First, we used eq 9 to express K_{Het} for mechanisms 1 and 2 (Figure 1).

$$K_{\mathrm{Het}} = \frac{[\mathrm{WT\text{-}ALS_{Het}}]^2}{[\mathrm{WT_{Hom}}]\cdot[\mathrm{ALS_{Hom}}]} \tag{9}$$

DOI: 10.1021/jacs.6b01742
J. Am. Chem. Soc. 2016, 138, 5351–5362

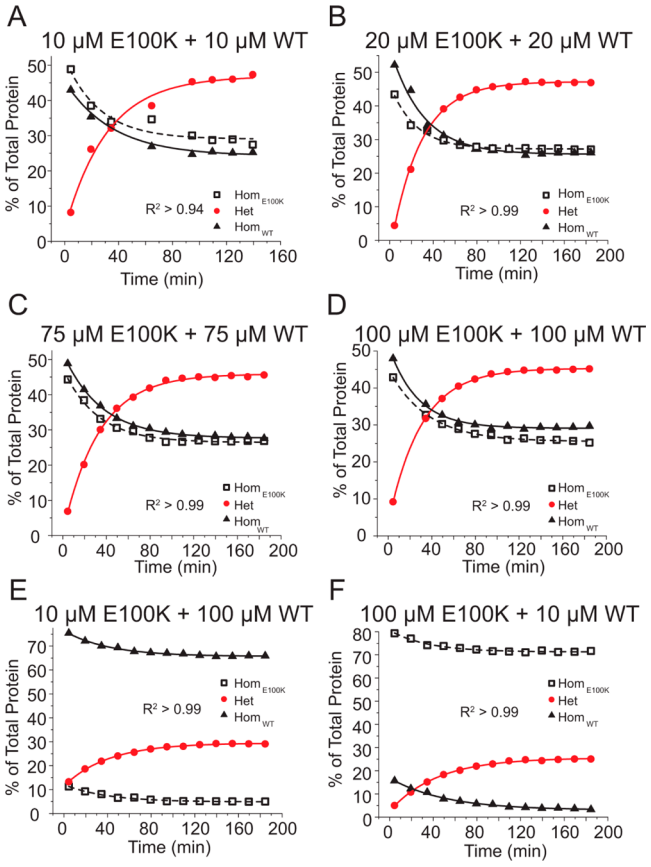

Figure 6. (A–F) Kinetic analysis of the subunit exchange reaction between E100K and WT apo-SOD1 at varying protein concentrations. The relative abundance of E100K homodimer (□), WT homodimer (▲), and WT/E100K heterodimer (red ●) was calculated from the electropherograms in Figure 5 and plotted against reaction time. Each data set was fit with an exponential function (eq 6; average $R^2 > 0.94$) yielding the kinetic parameters listed in Figure 7A.

The ΔG_{Het} can be then calculated according to eq 10.

$$\Delta G_{Het} = -RT \ln K_{Het} \quad (10)$$

The values of K_{Het} and ΔG_{Het} are listed in Table 3 for each heterodimer. Values of ΔG_{Het} were favorable (negative) for all SOD1 proteins and varied from −1.15 kJ mol^{-1} (E100K) to −2.97 kJ mol^{-1} (D101N). The equilibrium constant expression (K_{Het}) is derived from the following chemical equations:

$$2WT_{Hom} + 2ALS_{Hom} \underset{k_{-1}}{\overset{k_1}{\rightleftharpoons}} 2WTALS_{Het} + WT_{Hom} + ALS_{Hom} \quad (11)$$

$$WT_{Hom} + ALS_{Hom} \underset{k_{-1}}{\overset{k_1}{\rightleftharpoons}} 2WTALS_{Het} \quad (12)$$

Some equilibrium electropherograms of WT and ALS-variant apo-SOD1 appear to show an approximate ratio of 1:2:1 for Hom_{WT}:Het:Hom_{ALS}. This ratio might be assumed (albeit incorrectly) to lead to K_{Het} = 1 and ΔG_{Het} = 0 kJ/mol. This assumption would be correct if it were correct to treat WT and mutant SOD1 as thermodynamically equivalent (chemically identical) species. The mutant and WT homodimers must be, however, treated as chemically unique species (eqs 11 and 12) when writing the equilibrium expression for heterodimerization. In this scenario (eq 9), a perfect ratio of 1:2:1 for Hom_{WT}:Het:Hom_{ALS} would yield K_{Het} = 4 and ΔG_{Het} = −3.4 kJ/mol (which is in the range of our calculated values), not K_{Het} = 1 and ΔG_{Het} = 0 kJ/mol. An actual value of ΔG_{Het} = 0 kJ/mol would require ratios of exactly 1:1:1 (according to eq 9).

We have recently shown that electric field strength across the CE capillary (which is similar to field strengths across cellular membranes) causes monomerization of A4V Zn_4-SOD1, but not WT Zn_4-SOD1, or any other ALS-variant we have studied.[48] As a control to ensure that voltage-induced monomerization is not affecting heterodimerization, we performed heterodimerization experiments under different capillary voltages. ΔG_{Het} for D101N apo-SOD1 was altered only by 0.024 kJ mol^{-1}/kV (Figure S1), which indicates that

A

[E100K] + [WT]	k_{Het}; 10^{-2} min^{-1}	Rate at t = 0 min; (μM)
[10 μM] + [10 μM]	3.17 ± 0.38	0.20
[20 μM] + [20 μM]	3.65 ± 0.10	0.74
[75 μM] + [75 μM]	3.03 ± 0.08	2.05
[100 μM] + [100 μM]	3.32 ± 0.04	2.79
[10 μM] + [100 μM]	2.47 ± 0.07	0.49
[100 μM] + [10 μM]	2.31 ± 0.07	0.58

B

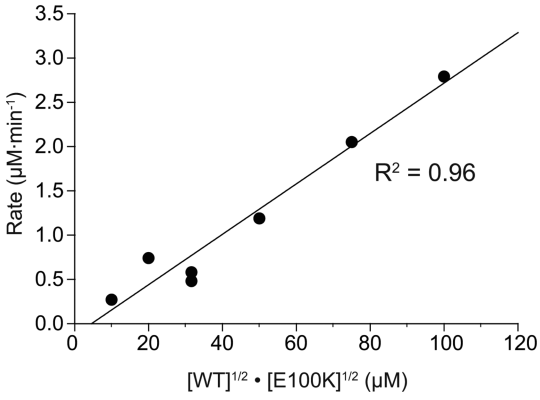

Figure 7. (A) Kinetic parameters for WT/ALS SOD1 heterodimerization at different concentrations of WT and E100K. (B) Comparison of heterodimerization rates as a function of concentration of E100K and WT apo-SOD1. The rates of the heterodimerization were plotted as a function of the square root of the product of [E100K apo-SOD1] and [WT apo-SOD1]. A linear fit yielded R^2 = 0.96.

Table 3. Melting Temperature (T_m) of Homodimeric Apo-SOD1 Proteins As Well As Calculated K_{Het} and ΔG_{Het} Values for Heterodimerization of WT and ALS-Variant Apo-SOD1 at 50 μM Homodimer, pH 7.4, 22 °C[a]

WT/ALS heterodimer	T_m homodimer (°C)	K_{Het}	ΔG_{Het} (kJ mol^{-1})
G37R	45.51	3.19 ± 0.06	−2.67 ± 0.04
N86D	49.62	2.97 ± 0.10	−2.51 ± 0.08
D90A	49.70	2.43 ± 0.08	−2.09 ± 0.11
G93R	44.42	2.73 ± 0.14	−2.31 ± 0.12
E100K	49.21	1.63 ± 0.04	−1.15 ± 0.03
E100G	43.51	3.37 ± 0.25	−2.86 ± 0.25
D101N	55.04	3.64 ± 0.22	−2.97 ± 0.13

[a]Values are shown as mean ± SD (n = 3).

DOI: 10.1021/jacs.6b01742
J. Am. Chem. Soc. 2016, 138, 5351−5362

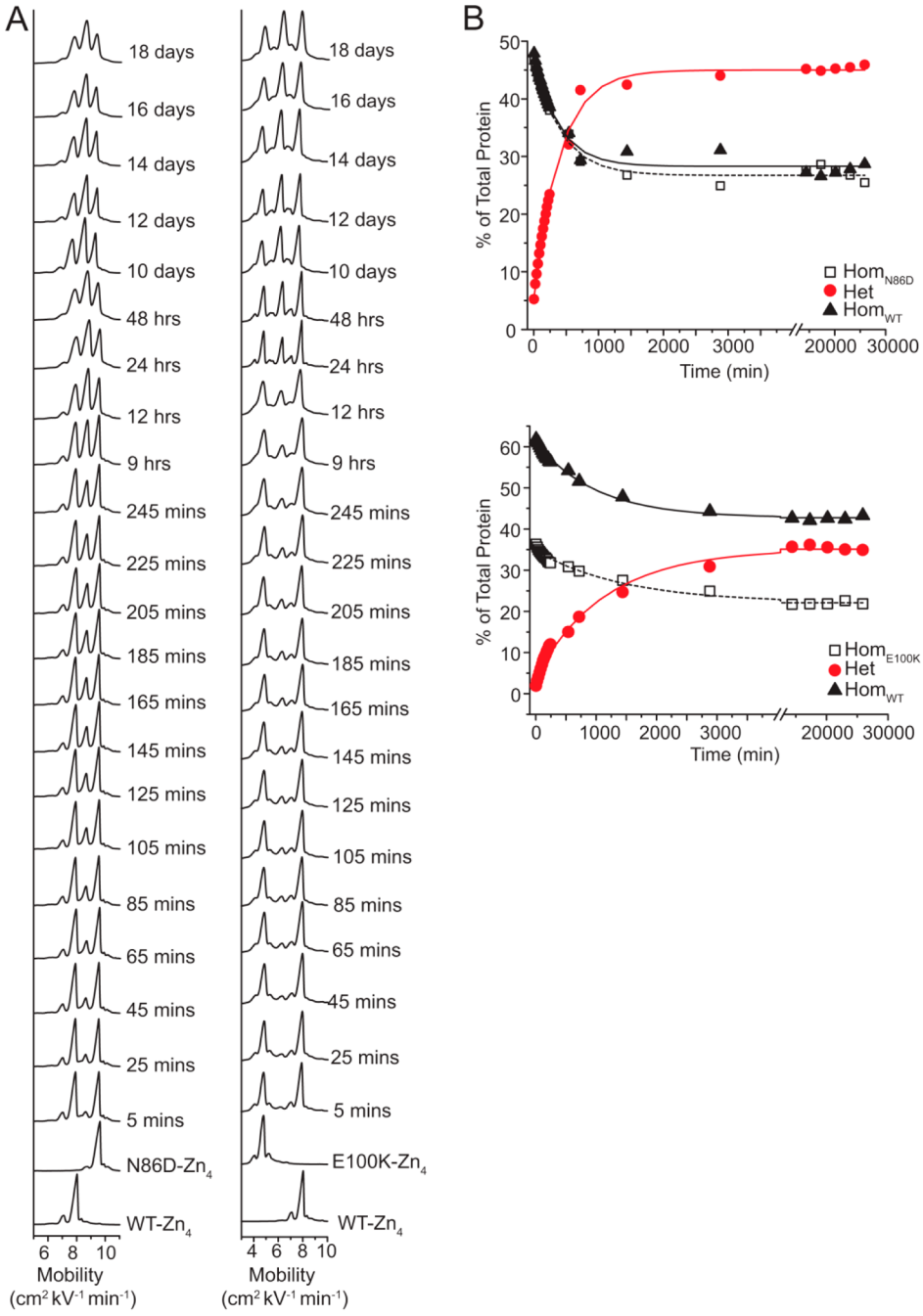

Figure 8. Heterodimerization between zinc-loaded ALS-variant and WT SOD1. (A) Capillary electropherograms of heterodimerization reactions between N86D Zn_4-SOD1, E100K Zn_4-SOD1, and WT Zn_4-SOD1 over time. (B) Quantification of heterodimerization for ALS-variant Zn_4 SOD1 and WT-Zn_4 SOD1 via analysis of electropherograms in part (A).

differences in capillary voltage do not contribute to variations in ΔG_{Het} observed for different mutants.

There is no clear correlation between the ΔG_{Het} and the thermostability of ALS SOD1 mutants (i.e., $R^2 < 0.001$). Thus, the ΔG_{Het} is driven by factors other than those that drive the thermostability of the respective homodimers. Moreover, the ΔG_{Het} of each ALS variant protein did not correlate with the rate of heterodimerization (i.e., $R^2 = 0.39$). Heterodimers of N86D and WT apo-SOD1 formed faster than G37R and WT despite the more favorable ΔG_{Het} of the WT/G37R heterodimer (Tables 2 and 3).

Metalation Significantly Decreases the Rate of Subunit Exchange, But Not ΔG_{Het}. We examined the kinetics of subunit exchange between a metalated (i.e., zinc-replete, Zn_4-SOD1) form of dimeric WT and ALS-variant SOD1. We chose to analyze zinc-loaded (Zn/Zn) SOD1, where zinc is coordinated to the copper and zinc site in each subunit (instead of Cu/Zn SOD1). This zinc loading prevents the possibility of mis-metalation. Zinc-loaded subunits are physiologically relevant[49] and have been detected in vivo.[40]

The rate and ΔG_{Het} of subunit exchange were measured for zinc-replete WT and five zinc-replete ALS-variant SOD1 proteins (chosen from the larger set of apo mutants per availability). CE electropherograms and integration plots of subunit exchange between WT Zn_4-SOD1 and two selected ALS-variant Zn_4-SOD1 proteins (N86D and E100K) are shown

DOI: 10.1021/jacs.6b01742
J. Am. Chem. Soc. 2016, 138, 5351−5362

Table 4. Kinetic and Thermodynamic Parameters of Heterodimerization for WT Zn_4-SOD1 and ALS-Variant Zn_4-SOD1 (50 μM homodimer, pH 7.4, 22 °C)[a]

WT/ALS heterodimer	rate constant (k; 10^{-2} min^{-1})	half-life ($t_{1/2}$; min)	rate (μM min^{-1}) at t = 0 min	K_{Het}	ΔG_{Het} (kJ mol^{-1})
N86D	0.24 ± 0.01	288.8 ± 8.1	0.05	2.75 ± 0.1	−2.33 ± 0.1
D90A	0.13 ± 0.01	533.2 ± 4.9	0.10	3.77 ± 0.2	−3.05 ± 0.1
G93R	0.33 ± 0.05	207.5 ± 19.8	0.12	2.05 ± 0.2	−1.65 ± 0.2
E100K	0.09 ± 0.01	770.2 ± 53.1	0.04	1.35 ± 0.1	−0.73 ± 0.1
D101N	0.26 ± 0.02	266.6 ± 14.2	0.11	2.63 ± 0.1	−2.39 ± 0.1

[a]Values are reported as mean ± SD (n = 3).

in Figure 8. All kinetic parameters of subunit exchange between zinc-replete SOD1 proteins are summarized in Table 4 as well as values for K_{Het} and ΔG_{Het}. Metalation slowed the rate of subunit exchange between WT and ALS-variant Zn_4-SOD1 by up to ~38-fold (Table 4). This decrease might be explained by the increased dimer stability of WT and mutant SOD1 upon binding metals.[50] Addition of zinc to SOD1 did not, however, alter the free energy of heterodimerization by a large magnitude (Table 4). For example, the maximum ΔG_{Het} variation was observed in the case of D90A SOD1 with a $\Delta\Delta G_{Het}$ = −0.96 ± 0.15 kJ mol^{-1}; that is, WT/D90A Zn_4-SOD1 was a more stable heterodimer than WT/D90A apo-SOD1 (Table 4).

CONCLUSION

This study demonstrated that heterodimerization occurs between dimeric WT and mutant apo-SOD1 and reaches equilibrium at time scales and protein concentrations (10−100 μM) that are physiologically relevant.[51] One limitation of this study is that we cannot distinguish between mechanism 1 (the dissociative mechanism) and mechanism 2 (the associative mechanism, Figure 1). Mechanism 1 would seem more probable because it involves a well-known intermediate (monomeric SOD1), while mechanism 2 involves a seemingly more obscure intermediate (a tetramer or higher order oligomer). Multiple studies have detected and studied monomeric SOD1,[51] while only one, that we can find, reports the existence of tetrameric SOD1.[52]

A simple comparison of heterodimerization rates with previously determined rates of monomerization and homodimerization for WT and ALS-variant apo-SOD1 might assist in discerning between mechanisms 1 and 2. For example, the estimated first-order rate constant of monomerization of an engineered form of WT apo-SOD1 (disulfide intact) is ~3-fold faster than the highest WT/mutant heterodimerization rate constant measured in this study (e.g., k_{Mono} = (9.73 ± 0.19) × 10^{-2} min^{-1}[27,53] vs k_{Het} for E100K = (3.89 ± 0.41) × 10^{-2} min^{-1}, Table 2), and redimerization rates for monomeric WT apo-SOD1 are nearly diffusion limited.[27] Moreover, the previously determined rate constant for D90A apo-SOD1 monomerization is ~12-fold higher than its rate constant for heterodimerization.[27] Thus, if mechanism 1 was operable, we would have expected to see faster rates of heterodimerization.

When considering that the rate of heterodmerization is directly proportional to the square root of the concentration of ALS-variant and WT apo-SOD1, mechanisms 1 and 2 are favored over mechanism 3 as the most likely pathways for subunit exchange between WT and ALS-variant apo-SOD1. The transient hetero-oligomer that would be formed during mechanism 2 would be forming continuously and frequently. Such species might provide a building block or point of genesis for the self-assembly of SOD1 into a toxic oligomer. It is possible that WT/ALS-variant heterodimerization could trigger a conformational change in either protein, or that WT SOD1 provides a template for the folding of intrinsically disordered ALS-variants, leading to the eventual self-assembly of misfolded SOD1. The plausibility of such a scenario is supported by a recent study of an engineered WT/ALS-variant covalent heterodimer (formed via a peptide linker).[16] The WT SOD1 subunit was observed to structurally order and increase the stability of the mutant SOD1 subunit in the covalent heterodimer.[16]

Although this study has shed light on the mechanism of SOD1 heterodimerization, much remains unknown regarding the structure, folding, and ligand- and metal-binding properties of heterodimeric SOD1. All structural analyses of ALS-variant SOD1, as well as other biophysical and biochemical analyses (e.g., rate and free energy of folding), were performed in the absence of WT SOD1.[19,20,25−27,53−56]

Previous studies have correlated the free energy of folding of some apo-SOD1 proteins with clinical phenotypes such as the survival time after diagnosis.[20] Generally, decreased SOD1 stability is associated with shorter survival times, but only for isoelectric mutant proteins.[20] The correlation is abolished when nonisoelectric mutations are included (especially D101N, which presents with a very short survival time, but has a free energy of folding almost identical to that of WT SOD1[20]). In the current study, we only examined nonisoelectric mutants of SOD1, because the heterodimerization of isoelectric ALS-variants and WT SOD1 cannot be easily measured using CE.

Incorporating the rate and free energy of SOD1 heterodimerization might improve correlations between clinical phenotype and the biophysical properties of ALS-variants.[20] We found no linear correlation between k_{Het} and either survival time (R^2 = 0.24) or age of onset of symptoms (R^2 = 0.11). A strong linear correlation was found, however, between the ΔG_{Het} and survival time after diagnosis for the variants that we studied (R^2 = 0.98; G37R was excluded from linear fits on the basis of its wide range of survival time of std dev ≈ ±12 yr) (Figure 9). Mutations with more favorable values of ΔG_{Het} (e.g., D101N) are associated with shorter survival time than those with less favorable values of ΔG_{Het} (e.g., D90A) by 4.8 yr/kJ (Figure 9).

The correlation between the ΔG_{Het} and survival time of a particular mutation is noteworthy because it can begin to explain why two similarly "cryptic" ALS-variants such as D90A and D101N SOD1[20,30,55] exhibit such drastically different clinical phenotypes.[20] The D101N mutation is known to have a more severe phenotype as compared to D90A, marked by a shorter survival time after onset of symptoms.[20] The more severe phenotype of D101N, as compared to D90A, cannot be explained by the thermostabilities of D101N and D90A apo-SOD1 because D101N apo-SOD1 is slightly more stable than D90A apo-SOD1 (Figure 9A). The two proteins also have otherwise similar biophysical and bioinorganic properties.[30,55]

DOI: 10.1021/jacs.6b01742
J. Am. Chem. Soc. 2016, 138, 5351−5362

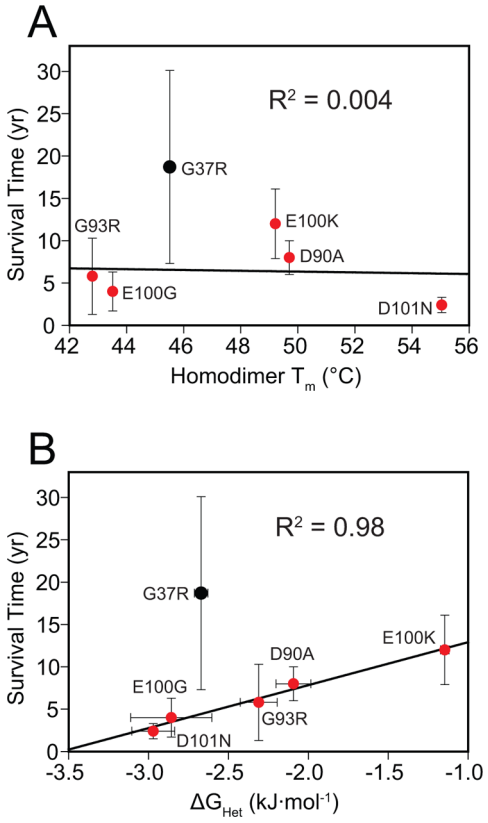

Figure 9. (A) There is no correlation between homodimer thermostability (T_m) of ALS-variant apo-SOD1 and patient survival. (B) Free energy of heterodimerization (ΔG_{Het}) shows a strong correlation with survival time after diagnosis. G37R was excluded from both plots A and B, on the basis of its wide range of survival times (SD $\approx \pm 12$ yr).

In fact, the ability of D101N substitution to promote heterodimerization, at equilibrium, more than D90A substitution is the only explanation that we can find for why the stable "WT-like" D101N SOD1 protein exhibits a more severe clinical phenotype than the equally less negatively charged, but still stable "WT-like" D90A SOD1 protein (Figure 9B).

The principal conclusion of this study is by no means that ΔG_{Het} can entirely explain, on a biophysical level, why one ALS mutation is more neurotoxic than another. Rather, the conclusion is that ΔG_{Het} varies with each mutation and is likely to be one predominant biophysical factor (of presumably many) in determining the toxicity of SOD1. The questions that immediately arise are why does the D101N amino acid substitution promote heterodimerization more than E100K? Why is the heterodimerization of D101N apo-SOD1 so much faster than N86D apo-SOD1? A first step in answering these kinetic and thermodynamic questions will require identification of the intramolecular and intermolecular forces that drive heterodimerization, and the measurement of ΔH_{Het} and calculation of ΔS_{Het}.

■ ASSOCIATED CONTENT

Supporting Information

The Supporting Information is available free of charge on the ACS Publications website at DOI: 10.1021/jacs.6b01742.

Further details on the derivation of rate law for different heterodimerization mechanisms, effect of capillary voltage on the heterodimerization of WT and D101N apo-SOD1 proteins, and supporting references (PDF)

■ AUTHOR INFORMATION

Corresponding Author

*bryan_shaw@baylor.edu

Author Contributions

†Y.S. and M.J.A. contributed equally to this work.

Notes

The authors declare no competing financial interest.

■ ACKNOWLEDGMENTS

Financial support for this research was provided to B.F.S. by the Department of Defense (ALS Therapeutic Idea Award; W81XWH-11-1-0790), the National Science Foundation (CAREER Award; CHE: 1352122), and the Welch Foundation (AA-1854).

■ REFERENCES

(1) Andersen, P. M.; Forsgren, L.; Binzer, M.; Nilsson, P.; Ala-Hurula, V.; Keranen, M. L.; Bergmark, L.; Saarinen, A.; Haltia, T.; Tarvainen, I.; Kinnunen, E.; Udd, B.; Marklund, S. L. *Brain* **1996**, *119*, 1153−1172.

(2) Chen, S.; Sayana, P.; Zhang, X.; Le, W. *Mol. Neurodegener.* **2013**, *8*, 1−15.

(3) Pasinelli, P.; Brown, R. H. *Nat. Rev. Neurosci.* **2006**, *7*, 710−723.

(4) Prudencio, M.; Durazo, A.; Whitelegge, J. P.; Borchelt, D. R. *Hum. Mol. Genet.* **2010**, *19*, 4774−4789.

(5) Witan, H.; Kern, A.; Koziollek-Drechsler, I.; Wade, R.; Behl, C.; Clement, A. M. *Hum. Mol. Genet.* **2008**, *17*, 1373−1385.

(6) Borchelt, D. R.; Guarnieri, M.; Wong, P. C.; Lee, M. K.; Slunt, H. S.; Xu, Z. S.; Sisodia, S. S.; Price, D. L.; Cleveland, D. W. *J. Biol. Chem.* **1995**, *270*, 3234−3238.

(7) Bruijn, L. I.; Houseweart, M. K.; Kato, S.; Anderson, K. L.; Anderson, S. D.; Ohama, E.; Reaume, A. G.; Scott, R. W.; Cleveland, D. W. *Science* **1998**, *281*, 1851−1854.

(8) Kim, J.; Lee, H.; Lee, J. H.; Kwon, D. Y.; Genovesio, A.; Fenistein, D.; Ogier, A.; Brondani, V.; Grailhe, R. *J. Biol. Chem.* **2014**, *289*, 15094−15103.

(9) Witan, H.; Gorlovoy, P.; Kaya, A. M.; Koziollek-Drechsler, I.; Neumann, H.; Behl, C.; Clement, A. M. *Neurobiol. Dis.* **2009**, *36*, 331−342.

(10) Xu, G.; Ayers, J. I.; Roberts, B. L.; Brown, H.; Fromholt, S.; Green, C.; Borchelt, D. R. *Hum. Mol. Genet.* **2015**, *24*, 1019−1035.

(11) Fukada, K.; Nagano, S.; Satoh, M.; Tohyama, C.; Nakanishi, T.; Shimizu, A.; Yanagihara, T.; Sakoda, S. *Eur. J. Neurosci.* **2001**, *14*, 2032−2036.

(12) Wang, L.; Deng, H. X.; Grisotti, G.; Zhai, H.; Siddique, T.; Roos, R. P. *Hum. Mol. Genet.* **2009**, *18*, 1642−1651.

(13) Deng, H. X.; Shi, Y.; Furukawa, Y.; Zhai, H.; Fu, R.; Liu, E.; Gorrie, G. H.; Khan, M. S.; Hung, W. Y.; Bigio, E. H.; Lukas, T.; Dal Canto, M. C.; O'Halloran, T. V.; Siddique, T. *Proc. Natl. Acad. Sci. U. S. A.* **2006**, *103*, 7142−7147.

(14) Gurney, M. E.; Pu, H.; Chiu, A. Y.; Dal Canto, M. C.; Polchow, C. Y.; Alexander, D. D.; Caliendo, J.; Hentati, A.; Kwon, Y. W.; Deng, H. X. *Science* **1994**, *264*, 1772−1775.

(15) Graffmo, K. S.; Forsberg, K.; Bergh, J.; Birve, A.; Zetterstrom, P.; Andersen, P. M.; Marklund, S. L.; Brannstrom, T. *Hum. Mol. Genet.* **2013**, *22*, 51−60.

(16) Weichert, A.; Besemer, A. S.; Liebl, M.; Hellmann, N.; Koziollek-Drechsler, I.; Ip, P.; Decker, H.; Robertson, J.; Chakrabartty, A.; Behl, C.; Clement, A. M. *Neurobiol. Dis.* **2014**, *62*, 479−488.

(17) Goda, S.; Takano, K.; Yamagata, Y.; Nagata, R.; Akutsu, H.; Maki, S.; Namba, K.; Yutani, K. *Protein Sci.* **2000**, *9*, 369−375.

DOI: 10.1021/jacs.6b01742
J. Am. Chem. Soc. 2016, 138, 5351−5362

(18) Krebs, M. R.; Wilkins, D. K.; Chung, E. W.; Pitkeathly, M. C.; Chamberlain, A. K.; Zurdo, J.; Robinson, C. V.; Dobson, C. M. *J. Mol. Biol.* **2000**, *300*, 541−549.
(19) Elam, J. S.; Taylor, A. B.; Strange, R.; Antonyuk, S.; Doucette, P. A.; Rodriguez, J. A.; Hasnain, S. S.; Hayward, L. J.; Valentine, J. S.; Yeates, T. O.; Hart, P. J. *Nat. Struct. Biol.* **2003**, *10*, 461−467.
(20) Bystrom, R.; Andersen, P. M.; Grobner, G.; Oliveberg, M. *J. Biol. Chem.* **2010**, *285*, 19544−19552.
(21) Svensson, A. E.; Osman, B.; Kayatekin, C.; Adefusika, J. A.; Zitzewitz, J. A.; Matthews, C. R. *PLoS One* **2010**, *5*, e10064.
(22) Proctor, E. A.; Fee, L.; Tao, Y.; Redler, R. L.; Fay, J. M.; Zhang, Y.; Lv, Z.; Mercer, I. P.; Deshmukh, M.; Lyubchenko, Y. L.; Dokholyan, N. V. *Proc. Natl. Acad. Sci. U. S. A.* **2016**, *113*, 614−619.
(23) Das, A.; Plotkin, S. S. *J. Mol. Biol.* **2013**, *425*, 850−874.
(24) Doucette, P. A.; Whitson, L. J.; Cao, X.; Schirf, V.; Demeler, B.; Valentine, J. S.; Hansen, J. C.; Hart, P. J. *J. Biol. Chem.* **2004**, *279*, 54558−54566.
(25) Hough, M. A.; Grossmann, J. G.; Antonyuk, S. V.; Strange, R. W.; Doucette, P. A.; Rodriguez, J. A.; Whitson, L. J.; Hart, P. J.; Hayward, L. J.; Valentine, J. S.; Hasnain, S. S. *Proc. Natl. Acad. Sci. U. S. A.* **2004**, *101*, 5976−5981.
(26) Khare, S. D.; Caplow, M.; Dokholyan, N. V. *Amyloid* **2006**, *13*, 226−235.
(27) Lindberg, M. J.; Bystrom, R.; Boknas, N.; Andersen, P. M.; Oliveberg, M. *Proc. Natl. Acad. Sci. U. S. A.* **2005**, *102*, 9754−9759.
(28) Broom, H. R.; Rumfeldt, J. A.; Vassall, K. A.; Meiering, E. M. *Protein Sci.* **2015**, *24*, 2081−2089.
(29) Dolnik, V. *Electrophoresis* **2008**, *29*, 143−156.
(30) Rodriguez, J. A.; Shaw, B. F.; Durazo, A.; Sohn, S. H.; Doucette, P. A.; Nersissian, A. M.; Faull, K. F.; Eggers, D. K.; Tiwari, A.; Hayward, L. J.; Valentine, J. S. *Proc. Natl. Acad. Sci. U. S. A.* **2005**, *102*, 10516−10521.
(31) Luchinat, E.; Barbieri, L.; Rubino, J. T.; Kozyreva, T.; Cantini, F.; Banci, L. *Nat. Commun.* **2014**, *5*, 5502.
(32) Banci, L.; Barbieri, L.; Bertini, I.; Luchinat, E.; Secci, E.; Zhao, Y.; Aricescu, A. R. *Nat. Chem. Biol.* **2013**, *9*, 297−299.
(33) Lushchak, V. I. *J. Amino Acids* **2012**, *2012*, 736837.
(34) Tohgi, H.; Abe, T.; Yamazaki, K.; Murata, T.; Ishizaki, E.; Isobe, C. *Neurosci. Lett.* **1999**, *260*, 204−206.
(35) Frutiger, K.; Lukas, T. J.; Gorrie, G.; Ajroud-Driss, S.; Siddique, T. *Amyotrophic Lateral Scler.* **2008**, *9*, 184−187.
(36) Grad, L. I.; Yerbury, J. J.; Turner, B. J.; Guest, W. C.; Pokrishevsky, E.; O'Neill, M. A.; Yanai, A.; Silverman, J. M.; Zeineddine, R.; Corcoran, L.; Kumita, J. R.; Luheshi, L. M.; Yousefi, M.; Coleman, B. M.; Hill, A. F.; Plotkin, S. S.; Mackenzie, I. R.; Cashman, N. R. *Proc. Natl. Acad. Sci. U. S. A.* **2014**, *111*, 3620−3625.
(37) Urushitani, M.; Sik, A.; Sakurai, T.; Nukina, N.; Takahashi, R.; Julien, J. P. *Nat. Neurosci.* **2006**, *9*, 108−118.
(38) Zhao, W.; Beers, D. R.; Henkel, J. S.; Zhang, W.; Urushitani, M.; Julien, J. P.; Appel, S. H. *Glia* **2010**, *58*, 231−243.
(39) Ilieva, H.; Polymenidou, M.; Cleveland, D. W. *J. Cell Biol.* **2009**, *187*, 761−772.
(40) Lelie, H. L.; Liba, A.; Bourassa, M. W.; Chattopadhyay, M.; Chan, P. K.; Gralla, E. B.; Miller, L. M.; Borchelt, D. R.; Valentine, J. S.; Whitelegge, J. P. *J. Biol. Chem.* **2011**, *286*, 2795−2806.
(41) Karch, C. M.; Prudencio, M.; Winkler, D. D.; Hart, P. J.; Borchelt, D. R. *Proc. Natl. Acad. Sci. U. S. A.* **2009**, *106*, 7774−7779.
(42) Shi, Y.; Mowery, R. A.; Shaw, B. F. *J. Mol. Biol.* **2013**, *425*, 4388−4404.
(43) Shi, Y.; Rhodes, N. R.; Abdolvahabi, A.; Kohn, T.; Cook, N. P.; Marti, A. A.; Shaw, B. F. *J. Am. Chem. Soc.* **2013**, *135*, 15897−15908.
(44) Shi, Y.; Abdolvahabi, A.; Shaw, B. F. *Protein Sci.* **2014**, *23*, 1417−1433.
(45) Mortensen, U. H.; Bendixen, C.; Sunjevaric, I.; Rothstein, R. *Proc. Natl. Acad. Sci. U. S. A.* **1996**, *93*, 10729−10734.
(46) Sobott, F.; Benesch, J. L.; Vierling, E.; Robinson, C. V. *J. Biol. Chem.* **2002**, *277*, 38921−38929.
(47) Wetmur, J. G. *Annu. Rev. Biophys. Bioeng.* **1976**, *5*, 337−361.
(48) Shi, Y.; Acerson, M. J.; Shuford, K. L.; Shaw, B. F. *ACS Chem. Neurosci.* **2015**, *6*, 1696−1707.
(49) Leinartaite, L.; Saraboji, K.; Nordlund, A.; Logan, D. T.; Oliveberg, M. *J. Am. Chem. Soc.* **2010**, *132*, 13495−13504.
(50) Potter, S. Z.; Zhu, H.; Shaw, B. F.; Rodriguez, J. A.; Doucette, P. A.; Sohn, S. H.; Durazo, A.; Faull, K. F.; Gralla, E. B.; Nersissian, A. M.; Valentine, J. S. *J. Am. Chem. Soc.* **2007**, *129*, 4575−4583.
(51) Rakhit, R.; Crow, J. P.; Lepock, J. R.; Kondejewski, L. H.; Cashman, N. R.; Chakrabartty, A. *J. Biol. Chem.* **2004**, *279*, 15499−15504.
(52) Allen, M. J.; Lacroix, J. J.; Ramachandran, S.; Capone, R.; Whitlock, J. L.; Ghadge, G. D.; Arnsdorf, M. F.; Roos, R. P.; Lal, R. *Neurobiol. Dis.* **2012**, *45*, 831−838.
(53) Lindberg, M. J.; Normark, J.; Holmgren, A.; Oliveberg, M. *Proc. Natl. Acad. Sci. U. S. A.* **2004**, *101*, 15893−15898.
(54) Kayatekin, C.; Zitzewitz, J. A.; Matthews, C. R. *J. Mol. Biol.* **2010**, *398*, 320−331.
(55) Shaw, B. F.; Valentine, J. S. *Trends Biochem. Sci.* **2007**, *32*, 78−85.
(56) Valentine, J. S.; Doucette, P. A.; Zittin Potter, S. *Annu. Rev. Biochem.* **2005**, *74*, 563−593.

DOI: 10.1021/jacs.6b01742
J. Am. Chem. Soc. 2016, 138, 5351−5362